

## Microstructure and room temperature mechanical properties of NiAl–Cr(Mo)–(Hf, Dy) hypoeutectic alloy prepared by injection casting

Li-yuan SHENG<sup>1,2</sup>, Fang YANG<sup>3</sup>, Ting-fei XI<sup>1</sup>, Yu-feng ZHENG<sup>2</sup>, Jian-ting GUO<sup>4</sup>

1. Shenzhen Institute, Peking University, Shenzhen 518057, China;

2. College of Engineering, Peking University, Beijing 100871, China;

3. Shenzhen Airline, Shenzhen Bao'an International Airport, Shenzhen 518128, China;

4. Institute of Metal Research, Chinese Academy of Sciences, Shenyang 110016, China

Received 9 March 2012; accepted 14 September 2012

**Abstract:** The NiAl–Cr(Mo)–(Hf,Dy) hypoeutectic alloys were prepared by conventional casting and injection casting techniques respectively, and their microstructure and room temperature mechanical properties were investigated. The results reveal that with the addition of Hf and Dy, the Ni<sub>2</sub>AlHf Heusler phase and Ni<sub>5</sub>Dy phase form along the NiAl/Cr(Mo) phase boundaries in intercellular region. By the injection casting method, some Ni<sub>2</sub>AlHf Heusler phase and Ni<sub>5</sub>Dy phase transform into Hf and Dy solid solutions, respectively. Moreover, the microstructure of the alloy gets good optimization, which can be characterized by the fine interlamellar spacing, high proportion of eutectic cell area and homogeneously distributed fine Ni<sub>2</sub>AlHf, Ni<sub>5</sub>Dy, Hf solid solution and Dy solid solutions. Compared with conventional-cast alloy, the room temperature mechanical properties of injection-cast alloy are improved obviously.

**Key words:** NiAl based hypoeutectic alloy; Hf; Dy; injection casting; microstructure; mechanical properties

### 1 Introduction

There has been an interest in developing alloys based on NiAl for high temperature structural applications in aircraft engines, since they possess many advantages such as high melting point, low density and excellent capacity of heat transmission [1–3]. However, the limited room temperature ductility and toughness as well as poor elevated temperature strength seriously handicap its commercial application [4,5]. Previous researches on NiAl revealed that the addition of refractory metals like V, Mo, Cr and Re can improve its room temperature (RT) toughness and elevated temperature strength simultaneously [6–10]. For example, a well directionally solidified NiAl–28Cr–6Mo (NiAl–Cr(Mo) for short) eutectic alloy yields a room temperature fracture toughness value of 21.5 MPa·m<sup>1/2</sup> [11], but its high temperature (HT) property is still poor [12,13]. Fortunately, recent studies have revealed that the minor addition of Hf can improve the HT property of the

alloy significantly [14,15]. Moreover, SHENG et al [16] found that the proper addition of rare earth (RE) elements could improve the mechanical properties of the Hf-doped NiAl–Cr(Mo) eutectic alloy further. However, the addition of Hf and RE could result in the formation of bulk hard phase along cell boundary, which is prone to be the origin of crack at RT and detrimental to its RT mechanical properties [17]. Therefore, in order to improve its RT mechanical properties, it is necessary to reduce or eliminate the segregation of Hf and RE and then decrease the hard phase on cell boundary.

To this kind of intermetallic based hypoeutectic alloy, the microstructural control is an excellent way to improve the ductility and toughness without deteriorating the strength of these materials. For NiAl–Cr(Mo) hypoeutectic alloy with strengthening precipitates, a possible way to improve its RT mechanical properties is to reduce the lamellar spacing and the segregation of strengthening precipitates. Recently, the investigations [18–20] on the strong magnetic field treated Hf-doped NiAl–Cr(Mo) eutectic alloy have revealed that improving

**Foundation item:** Project (2012M510271) supported by the China Postdoctoral Science Foundation; Project (2012BA118B05) supported by the Five-Year National Key Technology R&D Program during the 12th Five-year Plan of China; Project (2011AA030104) supported by the National High Technology Research and Development Program of China

**Corresponding author:** Li-yuan SHENG; Tel: +86-18665806226; Fax: +86-755-26984814; E-mail: lysheng@yeah.net  
DOI: 10.1016/S1003-6326(13)62556-X

the size and distribution of the strengthening precipitates in the alloy is beneficial to its RT mechanical properties. However, the limitations of the strong magnetic field treating equipment restrict its application. Compared with the strong magnetic field treatment, rapid solidification is another way, which is more feasible to attain the aim. As a kind of rapid solidification, injection casting is a popular method to fabricate metal glasses and can attain the high cooling rate about  $10^2$  K/s [21]. Furthermore, few studies have been done on the Hf- and Dy-doped NiAl–Cr(Mo) hypoeutectic alloy fabricated by injection casting. Therefore, in the present study, the Ni–33Al–28Cr–4Mo–0.25Hf–0.05Dy (mole fraction, %) alloy was prepared by the injection casting. Its microstructure and room temperature mechanical properties were investigated.

## 2 Experimental

The master alloy of Ni–33Al–28Cr–4Mo–0.25Hf–0.05Dy (mole fraction, %) (NiAl–Cr(Mo)–(Hf,Dy) for short) was prepared by vacuum induction furnace with starting materials of 99.99% Ni, 99.9% Al, 99.9% Cr, 99.9% Mo, 99.9% Hf and 99.9% Dy, respectively. The melted alloy was poured into the  $\text{Al}_2\text{O}_3$ – $\text{SiO}_2$  ceramic mold at about 0.3 m height. The pouring temperature was about 1800 K, which was a little higher than the melting point of the alloy (about 1700 K). The alloy rods prepared by conventional casting had a size of 50 mm in diameter and 300 mm in length. Some of them were investigated at as-cast state, and the others were crushed for injection casting. The injection casting was conducted by the water-cooled copper mold method, which had a significant undercooling capacity. The schematic diagram of the injection casting is shown in Fig. 1. Firstly, an appropriate amount of the alloy was melted again in quartz crucible under high vacuum and argon atmosphere. Then, the remelted alloy was injected with a nozzle into a copper mould by argon at a high speed of about 200 m/s. The copper mould had inner

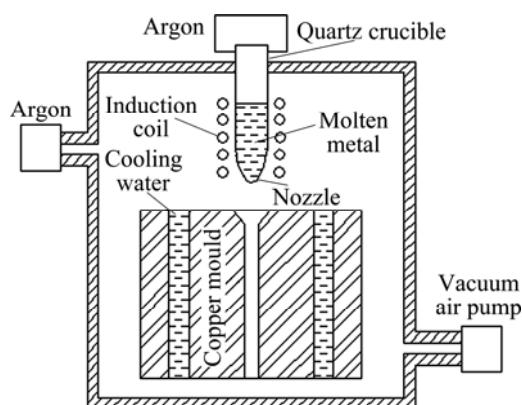


Fig. 1 Schematic diagram of injection casting apparatus

cavity with a size of  $d5$  mm $\times$ 80 mm and was cooled by high-speed water.

The microstructural characterization and the compressive sample fracture surface investigation of the alloys fabricated by conventional casting and injection casting were carried out by an S–3400 scanning electron microscope (SEM) with an energy-dispersive spectrometer (EDS). The compositions of the phases were detected by an EPMA–1610 electronic probe microanalyser (EPMA). The interlamellar spacing ( $\lambda$ ) of the alloys was measured by the line-intercept method at the eutectic cell interior. The region with a fine interlamellar spacing was defined as the size of eutectic cell, while the region between neighboring eutectic cells with a coarser interlamellar spacing was defined as the intercellular zone. The foils for transmission electron microscopy (TEM) observation were prepared by the conventional twin jet polishing technique using an electrolyte of 10% perchloric acid in methanol at  $-20$  °C after mechanical polishing to 50  $\mu\text{m}$  and cutting into disc with a diameter of 3.0 mm. The transmission electron microscopy observation was performed by a JEM–2010 transmission electron microscope operated at 200 kV.

The microhardness was obtained by an MHV–2000 Vickers microhardness tester at a load of 150 g and a dwell time of 15 s. Seven measurements were performed to evaluate an average value. The compressive specimens with a size of  $d5$  mm $\times$ 8 mm were cut from the conventional-cast and injection-cast alloys by electro-discharge machining (EDM) and all surfaces were mechanically ground with 600-grit SiC abrasive prior to compressive test. The compressive tests were conducted in a Gleeble–1500 test machine at room temperature and an initial strain rate of  $1\times 10^{-3}$  s $^{-1}$ .

## 3 Results and discussion

### 3.1 Microstructure characteristics

The typical microstructures of the conventional-cast NiAl–Cr(Mo)–(Hf,Dy) hypoeutectic alloy are shown in Fig. 2. It can be seen that the alloy is mainly composed of eutectic cell with an average size of 50  $\mu\text{m}$ , intercellular zone with the width of about 15  $\mu\text{m}$  and an amount of white phases distributed along the cell boundaries. The EDS analysis revealed that there are two kinds of white phases, one rich in Hf and the other rich in Dy. Both the white phases with irregular morphology distribute unevenly in the intercellular zone, which indicates a serious segregation of Hf and Dy elements. In the eutectic cells, black NiAl and gray Cr(Mo) plate phases exhibit the radially emanating pattern from the cell interior to the cell boundaries, while in the intercellular zone, coarse primary NiAl dendrites and Cr(Mo) phases exist with irregular forms. In the

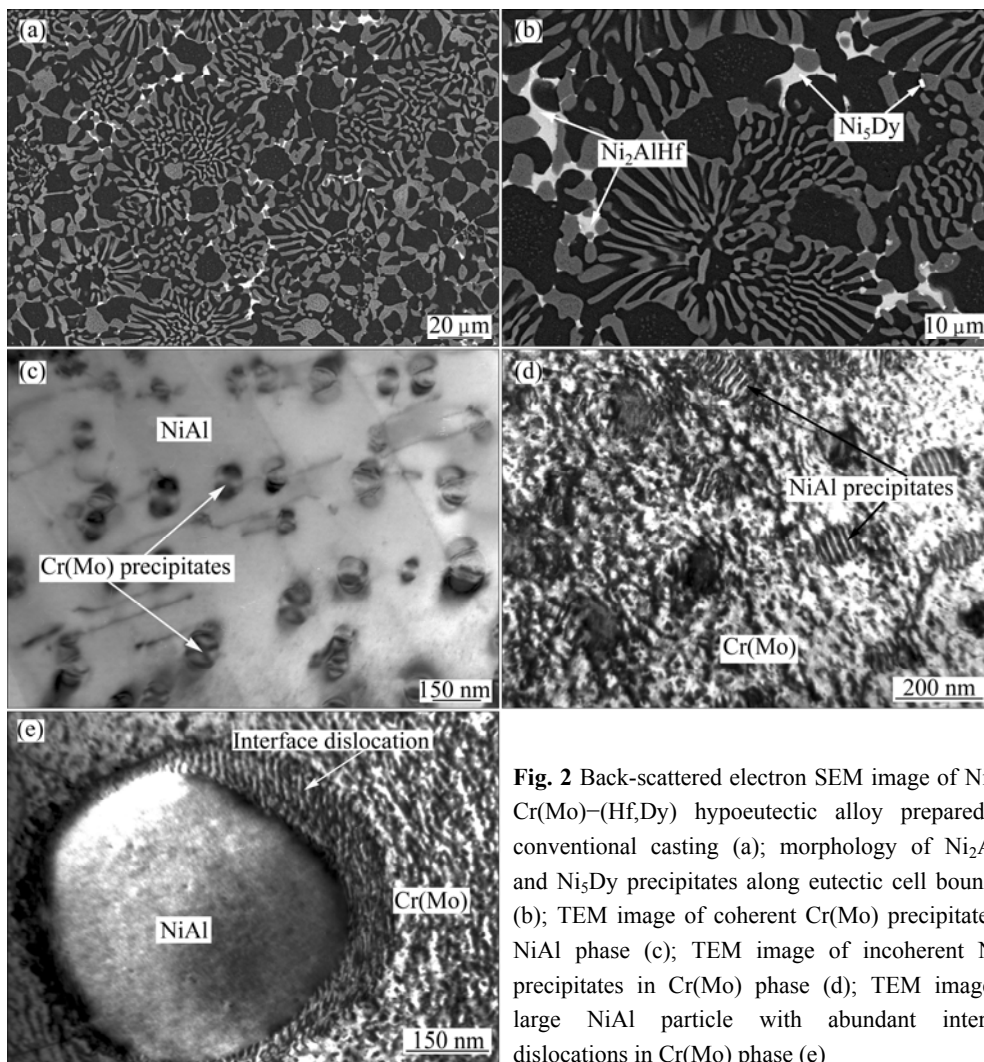


**Fig. 2** Back-scattered electron SEM image of NiAl–Cr(Mo)–(Hf,Dy) hypoeutectic alloy prepared by conventional casting (a); morphology of  $\text{Ni}_2\text{AlHf}$  and  $\text{Ni}_5\text{Dy}$  precipitates along eutectic cell boundary (b); TEM image of coherent Cr(Mo) precipitates in NiAl phase (c); TEM image of incoherent NiAl precipitates in Cr(Mo) phase (d); TEM image of large NiAl particle with abundant interface dislocations in Cr(Mo) phase (e)

primary NiAl phase, it can be found that many particles precipitate inside. TEM observation on the NiAl phase reveals that the small particles are rich in Cr and Mo and can be determined as Cr(Mo) precipitates, as shown in Fig. 2(c). The zero contrast lines in the middle of each Cr(Mo) precipitate implies that the fine Cr(Mo) precipitates should be coherent with NiAl phase. While in Cr(Mo) lamella, the incoherent NiAl particles are observed with full dislocation inside, as shown in Fig. 2(d). Additionally, large NiAl precipitate can also be found in Cr(Mo) phase with abundant interface dislocation, as shown in Fig. 2(e).

In order to identify the white phases, further TEM observation was carried out. Figure 3 exhibits the bright field TEM image of the white phases and their selected area electron diffraction (SAED) patterns. From the results, one of the observed white phase can be determined as  $\text{Ni}_2\text{AlHf}$  Heusler phase, which has a cubic crystal structure with  $a=0.6810$  nm and the space group of  $Fm\bar{3}m$ . The other white phase can be determined as  $\text{Ni}_5\text{Dy}$ , which has a hexagonal crystal structure with

$a=0.4856$  nm,  $c=0.3969$  nm and the space group of  $P6/mmm$ . The SAED pattern of  $\text{Ni}_2\text{AlHf}$  also exhibits that the  $\text{Ni}_2\text{AlHf}$  phase has an orientation relationship with NiAl matrix of  $[110]_{\text{NiAl}} // [110]_{\text{Ni}_2\text{AlHf}}$  and  $(00\bar{1})_{\text{NiAl}} // (00\bar{2})_{\text{Ni}_2\text{AlHf}}$ , which is in agreement with the previous research [22].

The typical microstructures of the injection-cast NiAl–Cr(Mo)–(Hf, Dy) hypoeutectic alloy are shown in Fig. 4. Apparently, the microstructure of the injection-cast alloy is quite different from that of the conventional-cast alloy, as a result of high cooling rate during injection casting. The average eutectic cell size in the injection-cast alloy, about  $25 \mu\text{m}$ , is smaller than that of the conventional-cast alloy. The interlamellar spacing ( $\lambda$ ) in eutectic cell interior of the injection-cast alloy is finer than that of the conventional-cast alloy, ranging from  $0.59$  to  $4.62 \mu\text{m}$ . The width of the intercellular region within  $2\text{--}3 \mu\text{m}$  for the injection-cast alloy is far narrower than that for the conventional-cast alloy  $15\text{--}25 \mu\text{m}$ . The primary NiAl dendrites in the injection-cast alloy with an average size of  $6 \mu\text{m}$  mainly distribute at

the eutectic cell interior or cell boundary. Moreover, the area fractions of primary NiAl phase and eutectic cell in the injection-cast alloy are both higher than those in the conventional-cast alloy.

In addition, by comparing Fig. 2(a) with Fig. 4, it is found that the white phases are distinctly fined and distribute evenly at the eutectic cell boundaries. However, the EDS tests reveal that except the Ni<sub>2</sub>AlHf Heusler phase and Ni<sub>5</sub>Dy phase, there are still some other phases. The TEM analysis confirms the results of the EDS tests, as shown in Fig. 5. The figures show the bright field TEM image of the new phases and their selected area electron diffraction (SAED) patterns. From the results, one of the phase is determined as Hf solid solution (Hfss) phase, which has a cubic crystal structure with  $a=0.4400$  nm and the space group of  $Fm\bar{3}m$ . The other phase is determined as Dy solid solution phase (Dyss), which has

a hexagonal crystal structure with  $a=0.3590$  nm,  $c=0.5647$  nm and the space group of  $P6_3/mmc$ . The existence of Hfss and Dyss phases may be attributed to the high cooling rate, which suppresses the element diffusion.

The microstructure changes of the injection-cast alloy comparing with that of the conventional-cast alloy can be mainly attributed to different cooling rates. Previously, RAJ and LOCCI [23] investigated the directionally solidified NiAl–Cr(Mo) eutectic alloy and concluded that the eutectic cell size and lamellar spacing decreased with increasing the growth rate from 12.7 to 508 mm/h and the average width of the intercellular region was essentially independent of growth rate. However, it is surprise to find that the high cooling rate distinctly decreased the width of the intercellular region in the present investigation. According to the recent

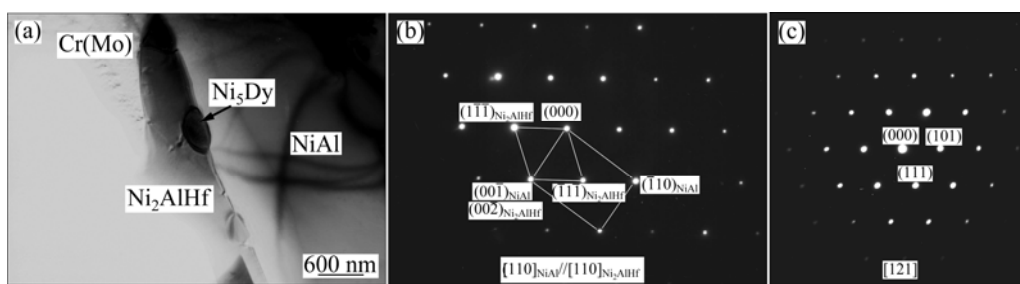


**Fig. 3** Bright field TEM image of Ni<sub>2</sub>AlHf and Ni<sub>5</sub>Dy phases (a); SAED pattern of Ni<sub>2</sub>AlHf phase along [110] zone axis (b); SAED pattern of Ni<sub>5</sub>Dy phase along [121] zone axis (c)

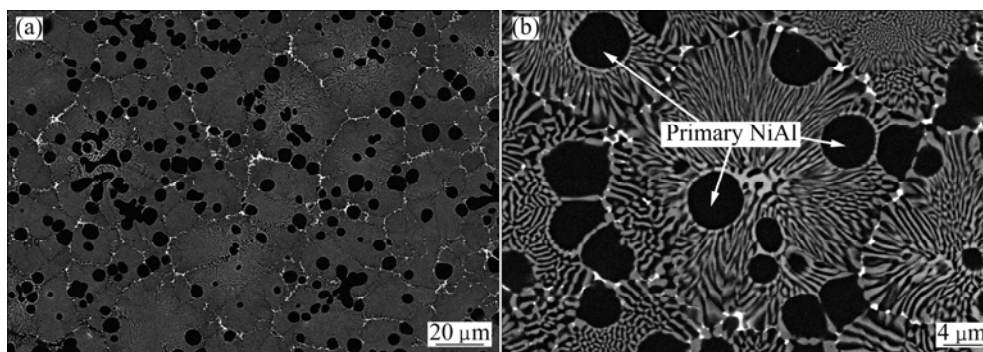


**Fig. 4** Back-scattered electron SEM images of NiAl–Cr(Mo)–(Hf,Dy) hypoeutectic alloy prepared by injection casting: (a) Low magnification; (b) High magnification



**Fig. 5** Bright field TEM image of Hfss and Dyss phases (a); SAED pattern of Hfss phase along [110] zone axis (b); SAED pattern of Dyss phase along [111] zone axis (c)

studies [24,25], the high cooling rate can generate great undercooling, which could increase the nucleation and then contribute to the eutectic cell refinement. In addition, the researches in Refs. [13,16] revealed that the rare earth element can arrest the impurities and act as the nucleation, which is also beneficial to the microstructural refinement. Furthermore, the large undercooling before the liquid/solid (L/S) interface will inevitably influence the growth of the crystal, which would make the growth velocity vertical to the L/S interface higher than that parallel to L/S interface. As a result, the NiAl and Cr(Mo) lamellas are refined greatly.

Further observation on the injection-cast alloy shows that there are abundant interface dislocation networks along the interfaces of NiAl and Cr(Mo) phases, as shown in Fig. 6. Such high-density interface dislocation networks well demonstrate the extension of solid solubility. EDS analysis reveals that the amount of Ni and Al solid solution in Cr(Mo) phase in the injection-cast alloy is higher than that of Cr and Mo in NiAl phase. There is no doubt that this will increase lattice misfit between the NiAl and Cr(Mo) phases and then result in more interface dislocations. PROBSTHEIN et al [26] studied the interface dislocation in the single crystal and concluded that the interface dislocations are beneficial to the mechanical properties. So it can be concluded that such abundant interface in the present investigation is beneficial to improving the strength of the injection-cast alloy. Moreover, a great amount of fine NiAl particles precipitate in the Cr(Mo) phase with an average size of 20 nm, which also demonstrates the high cooling rate inhibits element diffusions.

In order to study the effect of the injection casting on the NiAl–Cr(Mo)–(Hf,Dy) hypoeutectic alloy, the compositions of different phases in the alloy were detected, as shown in Table 1. The results show that the

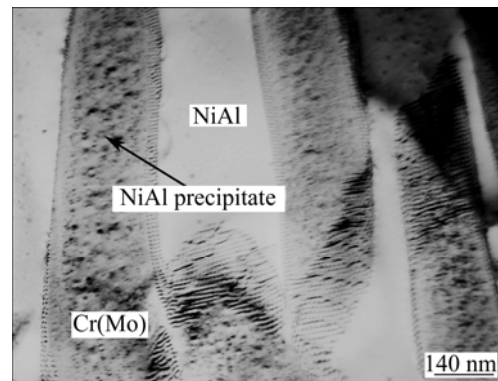


**Fig. 6** Misfit dislocation networks along NiAl and Cr(Mo) phase boundaries in injection-cast NiAl–Cr(Mo)–(Hf,Dy) hypoeutectic alloy

Cr content of primary NiAl phase in the injection-cast alloy increases greatly, more than four times of that in the conventional-cast one. Moreover, the Ni and Al contents in the Cr(Mo) phase increase significantly, compared with the conventional-cast alloy. Compared with the conventional-cast and injection-cast alloys, it can be found that the amount of Hf, Cr and Dy in Ni<sub>2</sub>AlHf phase increases obviously and the amount of Hf and Dy in Ni<sub>5</sub>Dy phase also increases a little. Such a change should be ascribed to the high cooling rate, which handicaps the element diffusion during the solidification.

### 3.2 Microhardness

The microhardness tests of the conventional-cast and the injection-cast alloys reveal that the hardness of primary NiAl in the injection-cast alloy is 20% higher than that in the conventional-cast alloy, as shown in Fig. 7. SONG et al [27] studied the site substitution of ternary elements in NiAl and concluded that Cr was mainly solid solution strengthening element in NiAl

**Table 1** Compositions of constituent phases in NiAl–Cr(Mo)–(Hf,Dy) hypoeutectic alloys fabricated by conventional casting and injection casting

Processing	Phase	Mole fraction/%					
		Ni	Al	Cr	Mo	Hf	Dy
Conventional-cast alloy	Primary NiAl	46.7	50.37	2.7	–	0.23	–
	Cr(Mo)	4.18	7.82	78	10	–	–
	Ni <sub>2</sub> AlHf	53.92	24.78	2.14	–	18.08	1.08
	Ni <sub>5</sub> Dy	57.80	20.63	2.61	–	0.58	18.38
Injection-cast alloy	Primary NiAl	46.17	44.14	9.10	–	0.43	0.16
	Cr(Mo)	16.69	15.92	62.60	4.79	–	–
	Ni <sub>2</sub> AlHf	48.46	22.35	3.64	–	24.24	2.31
	Ni <sub>5</sub> Dy	59.33	15.43	2.82	–	2.36	20.16
	Hfss	22.08	11.84	4.14	–	61.28	0.66
	Dyss	14.36	11.55	3.08	–	0.45	70.56

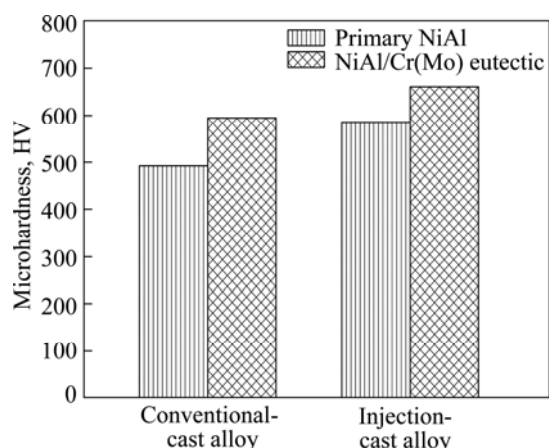


**Fig. 7** Microhardness of NiAl–Cr(Mo)–(Hf,Dy) hypoeutectic alloys prepared by conventional casting and injection casting

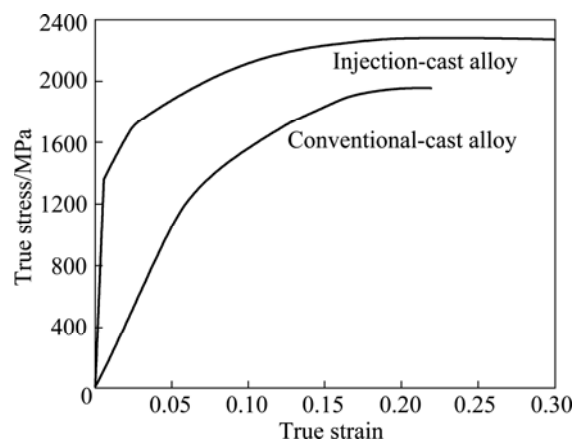
alloy and it preferred to occupying the site of Al. FROMMEYER et al [28] exhibited that the substitution of Cr for Al decreased the lattice parameter of NiAl slightly, which resulted in lattice distortion. In the injection-cast alloy, the 9% Cr solid solution in primary NiAl exceeds its solid solubility in equilibrium solidification state. So, the strengthening effects caused by the solid solution extension can result in the increase of the hardness of primary NiAl. Similar to the primary NiAl, the increase of hardness of NiAl/Cr(Mo) eutectic in the injection-cast alloy is obvious as well. Except the solid solution strengthening effect, the abundant interface dislocations can impede the dislocation movement, which can cooperate with the fine eutectic lamella to improve the microhardness of NiAl/Cr(Mo) eutectic.

### 3.3 Compressive properties

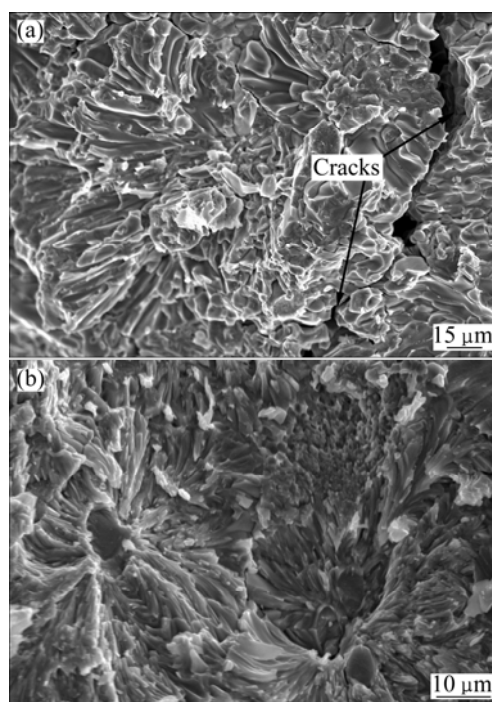
The true stress — true strain curves of the conventional-cast and injection-cast alloy at RT are shown in Fig. 8. These two kinds of alloys exhibit similar stress—strain curves with continuous hardening. Compared with the conventional-cast alloy, the RT compressive strain and yield strength of the injection-cast alloy are improved significantly to be 23% and 1362 MPa, respectively, which are increased by 75% and 50% over the conventional-cast alloy, indicating that the injection-cast technique is beneficial to improving the yield strength and compressive ductility. Additionally, the compressive strength of the injection-cast alloy increases to 2280 MPa, which is higher than that of the conventional-cast alloy.

Figure 9 shows the typical fractographs of the RT compressive samples. All the samples exhibit almost the similar fracture morphologies, which are composed of cleavage in primary NiAl and debonding along the NiAl/Cr(Mo) phase boundary inside the eutectic cell. The difference is that in the conventional-cast alloy there

are almost no cleavage fracture characteristics in the eutectic; while in the injection-cast alloy there are still many cleavage fractures in the eutectic lamella, and moreover some small dimple like features exist in the eutectic region. In addition, in the conventional-cast alloy there are obvious secondary cracks propagating along the eutectic cell boundary.



**Fig. 8** True stress—true strain curves of NiAl–Cr(Mo)–(Hf,Dy) hypoeutectic alloys prepared by conventional casting and injection casting



**Fig. 9** Typical fracture surfaces of compressive samples at RT: (a) Conventional-cast alloy; (b) Injection-cast alloy

Previous researches [29,30] showed that the cleavage traversing the eutectic lamella could take good advantage of the ductile Cr(Mo) phase and was beneficial to the ductility. Moreover, compared with conventional-cast alloy the disappearance of the crack along the eutectic cell boundaries in the injection-cast

alloy indicates that the adhesion of eutectic cell boundaries can be improved obviously. According with the recent studies on intermetallics [31,32], the oxides or impurities prefer to segregating along the grain and phase boundary. While in the present alloy these impurities would be expelled to the intercellular region during the solidification. Moreover, the addition of refractory elements can result in more impurities. Based on the previous research [33], these segregated impurities could form a film along the boundary, which would be the origin of crack. In the conventional-cast alloy, the slow cooling rate assists the impurity film to form and coarsen, which decreases the adhesion of the eutectic cell boundary. So there is no doubt that the crack always starts from the eutectic cell boundary. However, the high cooling rate reduces the segregation of impurities and then handicaps the formation and coarsening of the film. Such improvements contribute much to improving the adhesion of phases and eutectic cell boundaries. So, the cracks from the eutectic cell boundary are handicapped and the compressive ductility of the alloy is improved. The uniformly distributed fine  $\text{Ni}_2\text{AlHf}$ ,  $\text{Ni}_3\text{Dy}$ ,  $\text{Hfss}$  and  $\text{Dyss}$  phase particles are also beneficial to the compressive strength and ductility, because such size and distribution of the second phases reduce the stress concentration. In addition, the decrease of interlamellar spacing, the extended solubility and the increased area fraction of the eutectic cell contribute to improving the RT compressive strength of the injection-cast alloy.

## 4 Conclusions

1) With the addition of Hf and Dy elements in the NiAl–Cr(Mo)–(Hf,Dy) hypoeutectic alloy, the  $\text{Ni}_2\text{AlHf}$  Heusler phase and  $\text{Ni}_3\text{Dy}$  phase form along the NiAl/Cr(Mo) phases boundaries in the intercellular regions.

2) The injection-cast NiAl–Cr(Mo)–(Hf,Dy) alloy presents a fine microstructure, i.e., the refined eutectic cell size, interlamellar spacing, intercellular zone, which should be mainly attributed to the high cooling rate. In addition, the increase of solid solubility occurs in the alloy.

3) In the NiAl–Cr(Mo)–(Hf,Dy) alloy prepared by the injection casting, the high cooling rate results in the formation of some Hf and Dy solid solution phases. Moreover, the fine  $\text{Ni}_2\text{AlHf}$ ,  $\text{Ni}_3\text{Dy}$ , Hf solid solution and Dy solid solution particles distribute evenly along the eutectic cell boundary.

4) Compared with the conventional-cast NiAl–Cr(Mo)–(Hf,Dy) alloy, the yield strength and compressive ductility of the injection-cast alloy at room

temperature are improved significantly.

## References

- [1] MIRACLE D B. Overview No. 104 the physical and mechanical properties of NiAl [J]. *Acta Metallurgica et Materialia*, 1993, 41(3): 649–684.
- [2] GUO Jian-ting, ZHOU Lan-zhang, LI Gu-song. High temperature structural intermetallics and their strengthening-softening mechanisms [J]. *The Chinese Journal of Nonferrous Metals*, 2011, 21(1): 1–34. (in Chinese)
- [3] SHENG L Y, YANG F, GUO J T, YE H Q. Investigation on NiAl–TiC– $\text{Al}_2\text{O}_3$  composite prepared by self-propagation high temperature synthesis with hot extrusion [J]. *Composites Part B: Engineering*, 2013, 45(1): 785–791.
- [4] DAROLIA R. NiAl alloys for high temperature structural applications [J]. *Journal of Metal*, 1991, 43(3): 44–49.
- [5] SHENG Li-yuan, GUO Jian-ting, ZHANG Wei, ZHOU Lan-zhang, YE Heng-qiang. Effects of HIP and heat treatment on microstructure and compressive properties of rapidly solidified NiAl–Cr(Mo)–Hf eutectic alloy [J]. *Acta Metallurgica Sinica*, 2009, 45(9): 1025–1029. (in Chinese)
- [6] SHENG L Y, ZHANG W, GUO J T, ZHOU L Z, YE H Q. Effect of Au addition on the microstructure and mechanical properties of NiAl intermetallic compound [J]. *Intermetallics*, 2010, 18(4): 740–744.
- [7] SHENG L Y, YANG F, XI T F, ZHENG Y F, GUO J T. Improvement of compressive strength and ductility in NiAl–Cr(Nb)/Dy alloy by rapid solidification and HIP treatment [J]. *Intermetallics*, 2012, 27: 14–20.
- [8] SHENG L Y, YANG F, XI T F, GUO J T. Investigation on microstructure and wear behavior of the NiAl–TiC– $\text{Al}_2\text{O}_3$  composite fabricated by self-propagation high-temperature synthesis with extrusion [J]. *Journal of Alloys and Compounds*, 2013, 554: 182–188.
- [9] WAN Xiao-jun, LIN Jian-guo. Interfacial microstructure and chemical stability during diffusion bonding of single crystal  $\text{Al}_2\text{O}_3$ -fibres with Ni<sub>25</sub>.8Al<sub>9</sub>.6Ta<sub>8</sub>.3Cr matrix [J]. *Transactions of Nonferrous Metals Society of China*, 2011, 21(5): 1023–1028.
- [10] SHENG L Y, XIE Y, XI T F, GUO J T, ZHENG Y F, YE H Q. Microstructure characteristics and compressive properties of NiAl-based multiphase alloy during heat treatments [J]. *Materials Science and Engineering A*, 2011, 528(29–30): 8324–8331.
- [11] CHEN X F, JOHNSON D R, NOEBE R D, OLLIVER B F. Deformation and fracture of a directionally solidified NiAl–28Cr–6Mo eutectic alloy [J]. *Journal of Materials Research*, 1995, 10(5): 1159–1170.
- [12] SHENG L Y, GUO J T, ZHOU L Z, YE H Q. Microstructure and compressive properties of NiAl–Cr(Mo)–Dy near eutectic alloy prepared by suction casting [J]. *Materials Science and Technology*, 2010, 26(2): 164–168.
- [13] SHENG L Y, GUO J T, TIAN Y X, ZHOU L Z, YE H Q. Microstructure and mechanical properties of rapidly solidified NiAl–Cr(Mo) eutectic alloy doped with trace Dy [J]. *Journal of Alloy Compound*, 2009, 475(1–2): 730–734.
- [14] GUO J T, CUI C Y, QI Y H, YE H Q. Microstructure and elevated temperature mechanical behavior of cast NiAl–Cr(Mo) alloyed with Hf [J]. *Journal of Alloy Compound*, 2002, 343(1–2): 142–150.
- [15] SHENG L Y, ZHANG W, GUO J T, ZHOU L Z, YE H Q. Microstructure evolution and mechanical properties' improvement of NiAl–Cr(Mo)–Hf eutectic alloy during suction casting and subsequent HIP treatment [J]. *Intermetallics*, 2009, 17(12): 1115–1119.

- [16] SHENG L Y, WANG L J, XI T F, ZHENG Y F, YE H Q. Microstructure, precipitates and compressive properties of various holmium doped NiAl/Cr(Mo, Hf) eutectic alloys [J]. *Materials and Design*, 2011, 32(10): 4810–4817.
- [17] SHENG L Y, ZHANG W, GUO J T, YE H Q. Microstructure and mechanical properties of Hf and Ho doped NiAl–Cr(Mo) near eutectic alloy prepared by suction casting [J]. *Materials Characterization*, 2009, 60(11): 1311–1316.
- [18] SHENG L Y, GUO J T, REN W L, ZHANG Z X, REN Z M, YE H Q. Preliminary investigation on strong magnetic field treated NiAl–Cr(Mo)–Hf near eutectic alloy [J]. *Intermetallics*, 2011, 19(2): 143–148.
- [19] SHENG Li-yuan, GUO Jian-ting, ZHANG Wei, ZHOU Lan-zhang, YE Heng-qiang. Effect of high magnetic field treatment on the microstructure and mechanical property of NiAl–Cr(Mo)–0.2Hf eutectic alloy [J]. *Acta Metallurgica Sinica*, 2008, 44(5): 524–528. (in Chinese)
- [20] SHENG L Y, GUO J T, ZHOU L Z, YE H Q. The effect of strong magnetic field treatment on microstructure and room temperature compressive properties of NiAl–Cr(Mo)–Hf eutectic alloy [J]. *Materials Science and Engineering A*, 2009, 500(1–2): 238–243.
- [21] ZHU Z W, ZHANG H F, DING B Z, HU Z Q. Synthesis and properties of bulk metallic glasses in the ternary Ni–Nb–Zr alloy system [J]. *Materials Science and Engineering A*, 2008, 492(1–2): 221–229.
- [22] CHEN Yu-xi, CUI Chuan-yong, HE Lian-long, GUO Jian-ting, LI Dou-xing. The microstructure of a directionally solidified NiAl–Cr(Mo)–Hf alloy [J]. *Acta Metallurgica Sinica*, 1999, 35(9): 897–901. (in Chinese)
- [23] RAJ S V, LOCCI I E. Microstructural characterization of a directionally-solidified Ni–33 (at.%) Al–31Cr–3Mo eutectic alloy as a function of withdrawal rate [J]. *Intermetallics*, 2001, 9(3): 217–227.
- [24] SHENG L Y, ZHANG W, GUO J T, WANG Z S, YE H Q. Microstructure evolution and elevated temperature compressive properties of a rapidly solidified NiAl–Cr(Nb)/Dy alloy [J]. *Materials and Design*, 2009, 30(7): 2752–2755.
- [25] SHENG L Y, GUO J T, YE H Q. Microstructure and mechanical properties of NiAl–Cr(Mo)/Nb eutectic alloy prepared by injection-casting [J]. *Materials and Design*, 2009, 30(4): 964–969.
- [26] PROBST-HEIN M, DLOUHY A, EGgeler G. Interface dislocations in superalloy single crystals [J]. *Acta Materialia*, 1999, 47(8): 2497–2510.
- [27] SONG Y, GUO Z X, YANG R, LI D. First principles study of site substitution of ternary elements in NiAl [J]. *Acta Materialia*, 2001, 49(9): 1647–1654.
- [28] FROMMEYER G, FISCHER R, DEGES J, RABLBAUER R, SCHNEIDER A. APFIM investigations on site occupancies of the ternary alloying elements Cr, Fe, and Re in NiAl [J]. *Ultramicroscopy*, 2004, 101(2–4): 139–148.
- [29] YANG J M, JENG S M, BAIN K, AMATO R A. Microstructure and mechanical behavior of in-situ directional solidified NiAl/Cr(Mo) eutectic composite [J]. *Acta Materialia*, 1997, 45(1): 295–308.
- [30] SHENG L Y, GUO J T, XI T F, ZHANG B C, YE H Q. ZrO<sub>2</sub> strengthened NiAl/Cr(Mo,Hf) composite fabricated by powder metallurgy [J]. *Progress in Natural Science: Materials International*, 2012, 22(3): 231–236.
- [31] SHENG Li-yuan, XI Ting-fei, LAI Chen, ZHENG Yu-feng, GUO Jian-ting. Effect of extrusion process on microstructure and mechanical properties of Ni<sub>3</sub>Al–B–Cr alloy during self-propagation high-temperature synthesis [J]. *Transactions of Nonferrous Metals Society of China*, 2012, 22(3): 489–495.
- [32] SHENG L Y, YANG F, XI T F, GUO J T, YE H Q. Microstructure evolution and mechanical properties of Ni<sub>3</sub>Al/Al<sub>2</sub>O<sub>3</sub> composite during self-propagation high-temperature synthesis and hot extrusion [J]. *Materials Science and Engineering A*, 2012, 555(15): 131–138.
- [33] CAMPBELL J. Entrainment defects [J]. *Materials Science and Technology*, 2006, 22(2): 127–145.

## 喷铸工艺制备 NiAl–Cr(Mo)–(Hf,Dy) 亚共晶合金的组织及室温力学性能

盛立远<sup>1,2</sup>, 杨芳<sup>3</sup>, 奚廷斐<sup>1</sup>, 郑玉峰<sup>2</sup>, 郭建亭<sup>4</sup>

1. 北京大学 深圳研究院, 深圳 518057;
2. 北京大学 工学院, 北京 100871;
3. 深圳宝安国际机场 深圳航空有限责任公司, 深圳 518128;
4. 中国科学院 金属研究所, 沈阳 110016

**摘要:** 采用普通重力铸造和喷铸制备 NiAl–Cr(Mo)–(Hf,Dy)亚共晶合金, 研究两种工艺制备的合金的微观组织和室温力学性能。结果表明, Hf 和 Dy 元素的添加导致 Ni<sub>2</sub>AlHf Heusler 相和 Ni<sub>5</sub>Dy 相在 NiAl/Cr(Mo)相界面析出。喷铸工艺促使部分 Ni<sub>2</sub>AlHf Heusler 和 Ni<sub>5</sub>Dy 相分别转变为 Hf 固溶体和 Dy 固溶体相, 层片间距得到细化, 共晶胞的面积比以及均匀分布的 Ni<sub>2</sub>AlHf、Ni<sub>5</sub>Dy、Hf 固溶体和 Dy 固溶体相增加。对比普通铸造合金, 喷铸合金的室温性能得到明显提高。

**关键词:** NiAl 基亚共晶合金; 喷铸; 钎; 钨; 微观组织; 力学性能

(Edited by Wei-ping CHEN)